Biometrika (2013), **100**, 1, *pp.* 1–4

Printed in Great Britain
Advance Access publication on 30 June 2013

Supplementary Material for 'Composite likelihood estimation for the Brown–Resnick process'

BY R. HUSER AND A. C. DAVISON

Ecole Polytechnique Fédérale de Lausanne, EPFL-FSB-MATHAA-STAT, Station 8, 1015 Lausanne, Switzerland

Raphael.Huser@epfl.ch Anthony.Davison@epfl.ch

SUMMARY

This document contains details on the computation of the trivariate density for the Brown–Resnick process and supporting simulations and figures for the paper.

1. COMPUTATION OF THE TRIVARIATE DENSITY FOR THE BROWN–RESNICK PROCESS

In three dimensions, the exponent measure may be written as $V(z_1, z_2, z_3) = I_1/z_1 + I_2/z_2 + I_3/z_3$, where $I_k = \Phi_2\{x_k(z_1, z_2, z_3), y_k(z_1, z_2, z_3); R_k\}$ for some differentiable functions x_k and y_k of z_1, z_2, z_3 $(k = 1, 2, 3)$; see equation (2) of the paper. Therefore, since the trivariate distribution is $F(z_1, z_2, z_3) = \exp\{-V(z_1, z_2, z_3)\}$, the density $f(z_1, z_2, z_3)$ is

$$\begin{aligned} f(z_1, z_2, z_3) &= \frac{d^3}{dz_1 dz_2 dz_3} \exp\{-V(z_1, z_2, z_3)\} \\ &= (-V_{123} + V_1 V_{23} + V_2 V_{13} + V_3 V_{12} - V_1 V_2 V_3) \exp(-V), \end{aligned}$$

where the derivatives $V_1 = dV(z_1, z_2, z_3)/dz_1$, etc., are given by expressions such as

$$\begin{aligned} V_1 &= -z_1^{-2} I_1 + z_1^{-1} \frac{dI_1}{dz_1} + z_2^{-1} \frac{dI_2}{dz_1} + z_3^{-1} \frac{dI_3}{dz_1} \\ V_{12} &= -z_1^{-2} \frac{dI_1}{dz_2} + z_1^{-1} \frac{d^2 I_1}{dz_1 dz_2} - z_2^{-2} \frac{dI_2}{dz_1} + z_2^{-1} \frac{d^2 I_2}{dz_1 dz_2} + z_3^{-1} \frac{d^2 I_3}{dz_1 dz_2} \\ V_{123} &= -z_1^{-2} \frac{d^2 I_1}{dz_2 dz_3} + z_1^{-1} \frac{d^3 I_1}{dz_1 dz_2 dz_3} - z_2^{-2} \frac{d^2 I_2}{dz_1 dz_3} + z_2^{-1} \frac{d^3 I_2}{dz_1 dz_2 dz_3} - z_3^{-2} \frac{d^2 I_3}{dz_1 dz_2} + z_3^{-1} \frac{d^3 I_3}{dz_1 dz_2 dz_3}. \end{aligned}$$

By the chain rule, and writing $x_k = x_k(z_1, z_2, z_3)$, $y_k = y_k(z_1, z_2, z_3)$ for simplicity, we have for $k, s, t, u = 1, 2, 3$ that

$$\begin{aligned} I_k &= \Phi_2(x_k, y_k; R_k), \\ \frac{d}{dz_s} I_k &= \frac{d}{dx_k} \Phi_2(x_k, y_k; R_k) \frac{dx_k}{dz_s} + \frac{d}{dy_k} \Phi_2(x_k, y_k; R_k) \frac{dy_k}{dz_s}, \\ \frac{d^2}{dz_s dz_t} I_k &= \frac{d^2}{dx_k^2} \Phi_2(x_k, y_k; R_k) \frac{dx_k}{dz_s} \frac{dx_k}{dz_t} + \frac{d^2}{dx_k dy_k} \Phi_2(x_k, y_k; R_k) \left(\frac{dx_k}{dz_s} \frac{dy_k}{dz_t} + \frac{dx_k}{dz_t} \frac{dy_k}{dz_s} \right) \\ &\quad + \frac{d^2}{dy_k^2} \Phi_2(x_k, y_k; R_k) \frac{dy_k}{dz_s} \frac{dy_k}{dz_t} + \frac{d}{dx_k} \Phi_2(x_k, y_k; R_k) \frac{d^2 x_k}{dz_s dz_t} + \frac{d}{dy_k} \Phi_2(x_k, y_k; R_k) \frac{d^2 y_k}{dz_s dz_t}, \end{aligned}$$

$$
\begin{aligned}
\frac{d^3}{dz_s dz_t dz_u} I_k = & \frac{d^3}{dx_k^3}\Phi_2(x_k, y_k; R_k)\frac{dx_k}{dz_s}\frac{dx_k}{dz_t}\frac{dx_k}{dz_u} \\
& + \frac{d^3}{dx_k^2 dy_k}\Phi_2(x_k, y_k; R_k)\left(\frac{dx_k}{dz_s}\frac{dx_k}{dz_t}\frac{dy_k}{dz_u} + \frac{dx_k}{dz_s}\frac{dx_k}{dz_u}\frac{dy_k}{dz_t} + \frac{dx_k}{dz_t}\frac{dx_k}{dz_u}\frac{dy_k}{dz_s}\right) \\
& + \frac{d^3}{dx_k dy_k^2}\Phi_2(x_k, y_k; R_k)\left(\frac{dx_k}{dz_s}\frac{dy_k}{dz_t}\frac{dy_k}{dz_u} + \frac{dx_k}{dz_t}\frac{dy_k}{dz_s}\frac{dy_k}{dz_u} + \frac{dx_k}{dz_u}\frac{dy_k}{dz_s}\frac{dy_k}{dz_t}\right) \\
& + \frac{d^3}{dy_k^3}\Phi_2(x_k, y_k; R_k)\frac{dy_k}{dz_s}\frac{dy_k}{dz_t}\frac{dy_k}{dz_u} \\
& + \frac{d^2}{dx_k^2}\Phi_2(x_k, y_k; R_k)\left(\frac{dx_k^2}{dz_s dz_t}\frac{dx_k}{dz_u} + \frac{dx_k^2}{dz_s dz_u}\frac{dx_k}{dz_t} + \frac{dx_k^2}{dz_t dz_u}\frac{dx_k}{dz_s}\right) \\
& + \frac{d^2}{dx_k dy_k}\Phi_2(x_k, y_k; R_k)\left(\frac{dx_k^2}{dz_s dz_t}\frac{dy_k}{dz_u} + \frac{dx_k^2}{dz_s dz_u}\frac{dy_k}{dz_t} + \frac{dx_k^2}{dz_t dz_u}\frac{dy_k}{dz_s}\right. \\
& \qquad \left. + \frac{dx_k}{dz_s}\frac{dy_k^2}{dz_t dz_u} + \frac{dx_k}{dz_t}\frac{dy_k^2}{dz_s dz_u} + \frac{dx_k}{dz_u}\frac{dy_k^2}{dz_s dz_t}\right) \\
& + \frac{d^2}{dy_k^2}\Phi_2(x_k, y_k; R_k)\left(\frac{dy_k^2}{dz_s dz_t}\frac{dy_k}{dz_u} + \frac{dy_k^2}{dz_s dz_u}\frac{dy_k}{dz_t} + \frac{dy_k^2}{dz_t dz_u}\frac{dy_k}{dz_s}\right) \\
& + \frac{d}{dx_k}\Phi_2(x_k, y_k; R_k)\frac{d^3 x_k}{dz_s dz_t dz_u} + \frac{d}{dy_k}\Phi_2(x_k, y_k; R_k)\frac{d^3 y_k}{dz_s dz_t dz_u}.
\end{aligned}
$$

The derivatives of the bivariate normal cumulative distribution function are easily derived as

$$
\begin{aligned}
\frac{d}{dx}\Phi_2(x, y; \rho) &= \phi(x)\Phi\left\{\frac{y - \rho x}{(1-\rho^2)^{1/2}}\right\}, \\
\frac{d^2}{dx^2}\Phi_2(x, y; \rho) &= -\phi(x)x\Phi\left\{\frac{y - \rho x}{(1-\rho^2)^{1/2}}\right\} - \rho\phi_2(x, y; \rho), \\
\frac{d^2}{dxdy}\Phi_2(x, y; \rho) &= \phi_2(x, y; \rho), \\
\frac{d^3}{dx^3}\Phi_2(x, y; \rho) &= (x-1)\phi(x)\Phi\left\{\frac{y - \rho x}{(1-\rho^2)^{1/2}}\right\} + \rho\phi_2(x, y; \rho)\left(-x^2 + x + \frac{x - \rho y}{1-\rho^2}\right), \\
\frac{d^3}{dx^2 dy}\Phi_2(x, y; \rho) &= -\phi_2(x, y; \rho)\frac{x - \rho y}{1-\rho^2},
\end{aligned}
$$

with the others defined by symmetry, and the non-zero derivatives of $x_k(z_1, z_2, z_3)$ and $y_k(z_1, z_2, z_3)$ with respect to z_1, z_2, z_3 are given for $n = 1, 2, \ldots$ by

$$
\begin{aligned}
\frac{d^n x_1}{dz_1^n} &= (n-1)!(-z_1)^{-n}\gamma_{12}^{-1/2}, & \frac{d^n x_1}{dz_2^n} &= -(n-1)!(-z_2)^{-n}\gamma_{12}^{-1/2}, \\
\frac{d^n y_1}{dz_1^n} &= (n-1)!(-z_1)^{-n}\gamma_{13}^{-1/2}, & \frac{d^n y_1}{dz_3^n} &= -(n-1)!(-z_3)^{-n}\gamma_{13}^{-1/2}, \\
\frac{d^n x_2}{dz_1^n} &= -(n-1)!(-z_1)^{-n}\gamma_{12}^{-1/2}, & \frac{d^n x_2}{dz_2^n} &= (n-1)!(-z_2)^{-n}\gamma_{12}^{-1/2},
\end{aligned}
$$

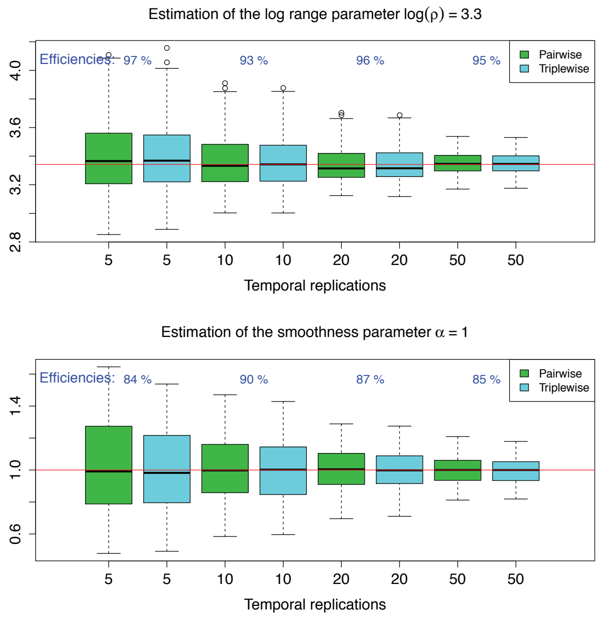

Fig. 1. Boxplots of the 300 independent estimates of the log-range parameter (top) and smooth parameter (bottom), as the number of temporal replicates n increases. Green and blue boxes correspond respectively to $\hat{\theta}_2$ and $\hat{\theta}_3$. The horizontal red lines correspond to the true values $\log(\rho) \approx 3.3$, i.e., $\rho = 28$, and $\alpha = 1$. The relative efficiencies $\hat{\mathrm{RE}}_\rho$ and $\hat{\mathrm{RE}}_\alpha$ are also reported.

$$\frac{d^n y_2}{dz_2^n} = (n-1)!(-z_2)^{-n}\gamma_{23}^{-1/2}, \qquad \frac{d^n y_2}{dz_3^n} = -(n-1)!(-z_3)^{-n}\gamma_{23}^{-1/2},$$

$$\frac{d^n x_3}{dz_1^n} = -(n-1)!(-z_1)^{-n}\gamma_{13}^{-1/2}, \qquad \frac{d^n x_3}{dz_3^n} = (n-1)!(-z_3)^{-n}\gamma_{13}^{-1/2}$$

$$\frac{d^n y_3}{dz_2^n} = -(n-1)!(-z_2)^{-n}\gamma_{23}^{-1/2}, \qquad \frac{d^n y_3}{dz_3^n} = (n-1)!(-z_3)^{-n}\gamma_{23}^{-1/2},$$

2. Supporting figures

Figure 1 below suggests that in a typical situation, with $\rho = 28$ and $\alpha = 1$, $\hat{\theta}_2$ and $\hat{\theta}_3$ estimate θ consistently as $n \to \infty$, and that their relative efficiency is quite stable with n. As Table 1 of the paper indicates, this is also true for other values of ρ and α, except for $\alpha = 2$. Figure 2 below illustrates the super-efficiency of $\hat{\theta}_3$ when $\alpha = 2$. Figure 3 suggests that the correlation matrices R_k in expression (2) of the paper may be numerically singular when $\alpha \approx 2$, especially for large p. In fact, they are exactly singular when $\alpha = 2$ and $p > d + 1$.

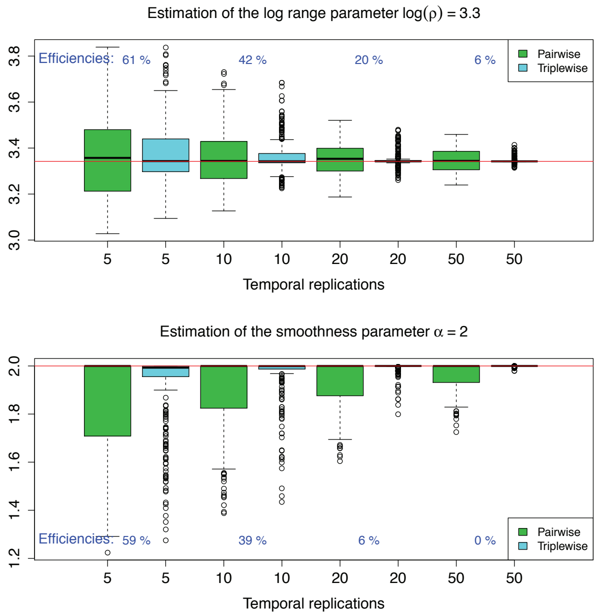

Fig. 2. Boxplots of the 300 independent estimates of the log-range parameter (top) and smooth parameter (bottom), as the number of temporal replicates n increases. Green and blue boxes correspond respectively to $\hat{\theta}_2$ and $\hat{\theta}_3$. The horizontal red lines correspond to the true values $\log(\rho) \approx 3.3$, i.e., $\rho = 28$, and $\alpha = 2$. The relative efficiencies $\hat{\mathrm{RE}}_\rho$ and $\hat{\mathrm{RE}}_\alpha$ are also reported.

3. EFFICIENCIES WITH INCREASING NUMBER OF LOCATIONS

Table 1 below suggests that when $\alpha < 2$, the efficiency of triplewise likelihood estimators is rather stable with the number of locations S, but when $\alpha = 2$, corresponding to the Smith model, the efficiency decreases rapidly with S; presumably this is also the case when $\alpha \approx 2$.

ACKNOWLEDGEMENT

This research was funded by the Swiss National Science Foundation, and partly performed in the context of the ETH Competence Center Environment and Sustainability (CCES).

[*Received January* 2011. *Revised June* 2011]

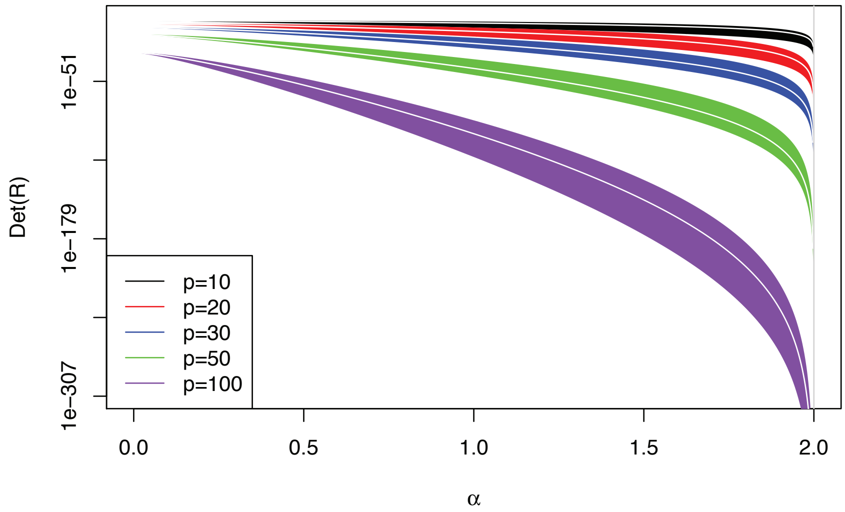

Fig. 3. Determinant of the correlation matrix R_1 in expression (2) of the paper against the smoothness parameter $\alpha \in (0, 2]$ when the range parameter ρ equals 100, for $d = 2$ and $p = 10$ (black), 20 (red), 30 (blue), 50 (green) and 100 (purple). The colored areas correspond to 95% confidence regions, while the white lines denote the medians based on 50 simulated locations in $[0, 100]^2$.

Table 1. *Efficiency (%) of maximum pairwise likelihood estimators relative to maximum triplewise likelihood estimators for $n = 20$, based on 300 simulations of the Brown–Resnick process with semi-variogram $(\|h\|/\rho)^\alpha$ observed at $S = 10, 20, 30, 50$ random sites in $[0, 100]^2$. The numbers are respectively $\mathrm{RE}_\rho/\mathrm{RE}_\alpha/\mathrm{RE}_\theta$.*

	$S = 10$			$S = 20$		
$\alpha \setminus \rho$	14	28	42	14	28	42
0.5	97/96/96	93/92/92	94/97/95	95/94/93	93/96/95	93/96/94
1.0	94/85/90	95/84/89	96/86/91	94/85/90	95/89/93	95/90/93
1.5	88/83/88	92/64/74	91/64/74	92/78/85	91/68/76	89/69/77
2.0	75/75/75	42/37/36	26/14/15	55/62/56	24/19/21	11/0/2

	$S = 30$			$S = 50$		
$\alpha \setminus \rho$	14	28	42	14	28	42
0.5	91/93/92	90/92/92	89/95/92	89/93/91	88/93/91	89/94/92
1.0	98/86/92	95/84/90	92/87/92	96/84/90	94/87/93	93/90/93
1.5	94/81/86	92/70/78	89/72/79	96/77/84	90/69/81	88/67/79
2.0	54/50/50	24/9/12	9/0/2	47/39/41	15/4/7	5/0/1